

See discussions, stats, and author profiles for this publication at: <https://www.researchgate.net/publication/337590741>

# The Raman spectrometer onboard the MMX rover for Phobos

Conference Paper · October 2019

CITATIONS

0

READS

296

8 authors, including:



**Pablo Rodríguez**

Instituto Nacional de Técnica Aeroespacial

36 PUBLICATIONS 334 CITATIONS

[SEE PROFILE](#)



**S. Ulamec**

German Aerospace Center (DLR)

382 PUBLICATIONS 2,811 CITATIONS

[SEE PROFILE](#)

Some of the authors of this publication are also working on these related projects:



Asteroid Impact Mission ([www.esa.int/aim](http://www.esa.int/aim)) [View project](#)



Solar Power Sail to Jupiter Trojans [View project](#)

IAC-19-A3.4.9

### The Raman spectrometer onboard the MMX rover for Phobos

**Till Hagelschuer<sup>a\*</sup>, Ute Böttger<sup>a</sup>, Maximilian Buder<sup>a</sup>, Yuichiro Cho<sup>b</sup>, Enrico Dietz<sup>a</sup>, Michael Gensch<sup>a</sup>, Franziska Hanke<sup>a</sup>, Heinz-Wilhelm Hübers<sup>a</sup>, Shingo Kameda<sup>c</sup>, Emanuel Kopp<sup>a</sup>, Simon Kubitz<sup>a</sup>, Andoni Moral<sup>d</sup>, Carsten Paproth<sup>a</sup>, Martin Pertenais<sup>a</sup>, Gisbert Peter<sup>a</sup>, Kristin Rammelkamp<sup>a</sup>, Pablo Rodriguez<sup>d</sup>, Fernando Rull<sup>e</sup>, Conor Ryan<sup>a</sup>, Thomas Säuberlich<sup>a</sup>, Friedrich Schrandt<sup>a</sup>, Susanne Schröder<sup>a</sup>, Stephan Ulamec<sup>f</sup>, Tomohiro Usui<sup>g</sup>, and Roderick Vance<sup>a</sup>**

<sup>a</sup> German Aerospace Center (DLR), Institute of Optical Sensor Systems, Rutherfordstraße 2, 12489 Berlin, Germany

<sup>b</sup> Department of Earth and Planetary Science, The University of Tokyo, 7-3-1 Hongo, Bunkyo, Tokyo 113-0033, Japan

<sup>c</sup> Department of Physics, College of Science, Rikkyo University, 3-34-1 Nishiikebukuro, Toshima, Tokyo 171-8501, Japan

<sup>d</sup> Instituto Nacional de Técnica Aeroespacial (INTA), Ctra. Ajalvir, Km 4, 28850 Torrejón de Ardoz, Spain

<sup>e</sup> Universidad de Valladolid –Unidad Asociada UVA-CSIC Centre de Astrobiología, Av. Francisco valles, 8, Parque Tecnológico de Boecillo, Parcela 203, E-47151 Boecillo, Valladolid, Spain

<sup>f</sup> German Aerospace Center (DLR), Microgravity User Support Center, Linder Höhe, 51147 Cologne, Germany

<sup>g</sup> Japan Aerospace Exploration Agency (JAXA), Institute of Space and Astronautical Science, Department of Solar System Sciences, 3-1-1 Yoshinodai, Chuo, Sagami-hara, Kanagawa, 252-5210, Japan

\* Till.Hagelschuer@dlr.de

#### Abstract

We present the Raman spectrometer onboard the rover which will be part of JAXA's Martian Moons eXploration (MMX) mission, to be launched in 2024. The “Raman for MMX” (RAX) instrument is designed to investigate the surface mineralogy of Phobos, according to the top-level science objectives of the MMX mission as defined by JAXA. The RAX instrument includes a laser, which has been developed for the Raman Laser Spectrometer (RLS) onboard the ExoMars rover to be launched in 2020, a very compact and highly sophisticated optical assembly, and a lightweight, space-qualified CMOS detector. The whole spectrometer requires a volume of only approximately  $81 \times 125 \times 98 \text{ mm}^3$  and has a mass of less than 1.4 kg. In-situ measurements of Raman spectra at different locations on Phobos will be realized by autonomously focusing the laser beam onto the ground below the rover. A calibration target is mounted inside the rover to provide frequency calibration prior to the measurements. This allows the identification of minerals on the surface of Phobos, validated by spectral analysis as well as by comparison with ground experiments and spectral laboratory reference data bases. The acquired data will be compared with the results obtained during the ExoMars2020 mission on the surface of Mars and thus help to better understand the origin of its moons.

**Keywords:** Raman spectroscopy, space technology, miniaturized optics, remote sensing, Martian moons

#### 1. Introduction

Space exploration using Raman spectroscopy in the visible spectral region has seen an increasing interest in recent years [1]. The Raman technique allows for analysing the vibrational mode of a substance either in solid, liquid or gaseous state and is therefore a powerful tool, especially in the field of planetary research. It relies on inelastic photon scattering (Raman scattering), which occurs when light impinges on an atom or molecule. The light-matter interaction gives rise to the Raman effect, where a significant energy shift of the exciting photons is observed. This “Raman-shift” appears as a spectral distribution with a fingerprint-like signature, which can be exploited for the unique

identification and structural analysis of substances, such as water-bearing minerals and organics.

Due to its significance, several space missions are already being prepared with Raman spectrometers. A prominent example is the SuperCam instrument onboard NASA's Mars 2020 rover mission [2]. In addition to a stand-off Raman spectrometer in a time-resolved configuration, which is capable of identifying geological and biological minerals up to a Raman-shift of  $4200 \text{ cm}^{-1}$  with a spectral resolution of  $< 10 \text{ cm}^{-1}$ , SuperCam integrates several other types of techniques such as Laser-Induced Breakdown Spectroscopy (LIBS), time-resolved luminescence, and visible and infrared reflectance spectroscopy. Another example is the Raman Laser Spectrometer (RLS) instrument onboard ESA's ExoMars 2020 rover mission [3]. The

RLS instrument is designed for investigating samples from beneath the Martian surface obtained with a drill and prepared inside the rover for analysis. RLS covers a spectral range of up to  $3800\text{ cm}^{-1}$  with a spectral resolution of  $< 8\text{ cm}^{-1}$ . It is based on a transmission spectrograph coupled to a CCD detector, an electronics box which includes the excitation laser and controls the instrument functions, and an optical head with an autofocus mechanism for illumination of the sample and collection of the scattered Raman light. Despite its complexity, the whole instrument including these three units weighs only approximately 2.3 kg. However, the increasing costs of space missions and the availability of compact and lightweight service modules with decreasing payload budgets pose a key challenge in reducing mass, volume and power consumption of a Raman system to a physical minimum.

In this article, we report on the design and performance of a compact Raman Spectrometer, which is developed for JAXA's Martian Moons eXploration (MMX) sample return mission to Phobos and Deimos (launch date: 2024). The "Raman for MMX" (RAX) instrument is a payload onboard the MMX rover (total mass:  $\sim 29.1\text{ kg}$ ; payload mass:  $\sim 2.6\text{ kg}$ ), which shall land on Phobos prior to the mothership. It is designed to identify Phobos' surface mineralogy, which is a top-level science objective of the overall MMX mission. The optical design of the RAX instrument includes a miniaturized laser unit emitting at 532 nm, which has been originally developed for the RLS instrument, a very compact and highly sophisticated confocal optical assembly, and a lightweight, space-qualified CMOS detector. It covers a spectral range of up to  $4000\text{ cm}^{-1}$  with a spectral resolution of approximately  $10\text{ cm}^{-1}$ . The whole spectrometer requires a volume of only approximately  $81 \times 125 \times 98\text{ mm}^3$  and has a mass of less than 1.4 kg. In order to perform in-situ measurements at different locations on Phobos, RAX has an integrated autofocus mechanism, which is used for precise focusing of the laser beam onto the ground below the rover. The Raman spectra obtained during the MMX rover mission can be directly compared with the results obtained by the RLS instrument on the Martian surface and with Raman measurement on the returned samples in Earth laboratories. This has the potential to reveal the genesis of Mars and one of its two moons.

## 2. RAX Scientific Objectives

The RAX scientific objectives are defined according to the science objectives of the MMX mission and the rover objectives. The latter include the surface analysis on Phobos (e.g. determination of the mineral/elemental distribution and grain size) as well as risk mitigation for the MMX lander. In order to achieve these goals, the RAX instrument should fulfil the following tasks during the mission:

- Investigation of the surface mineralogy on Phobos by spectroscopic identification
- Investigation of surface heterogeneities by visiting different locations on Phobos
- Supporting the characterisation of the landing site
- If possible, support the selection of samples for the return to Earth
- Comparison of RAX and RLS scientific measurements

The primary objective of the RAX instrument is the investigation of the surface mineralogy on Phobos by spectral identification using Raman spectroscopy.

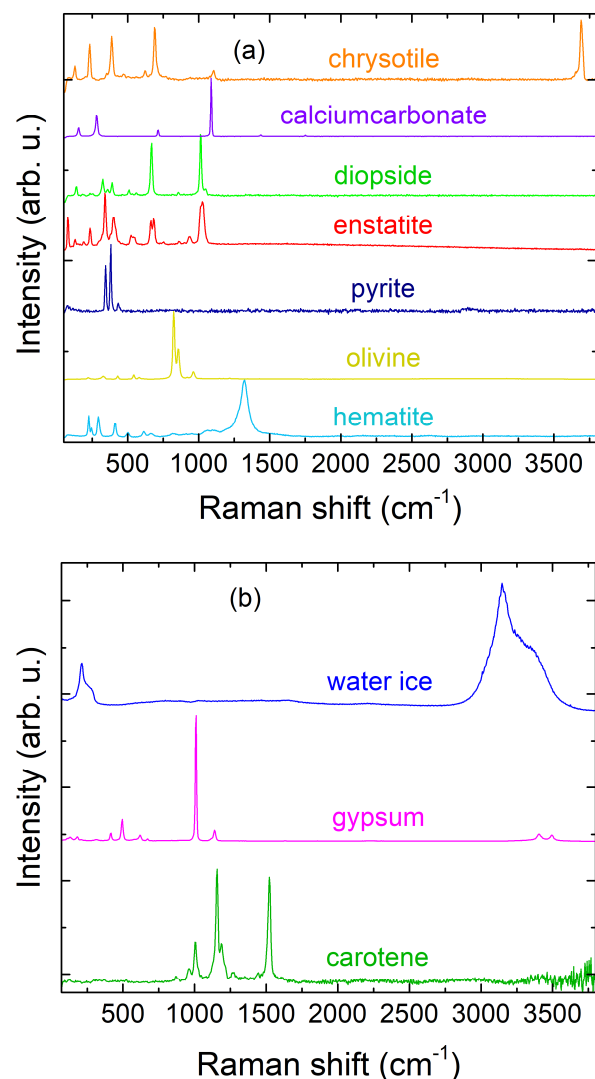


Fig. 1(a). Raman spectra of typical minerals expected on Phobos. The samples have been chosen according to the Planetary Simulant Database. (b) Raman spectra of samples possibly related to the presence of pure water and biologic material.

Figure 1(a) presents several Raman spectra of samples which are possibly expected on Phobos. The spectra have been measured with a confocal Raman microscope system (WiTEC) with a continuous wave (cw) 532 nm laser in the spectral range of  $50\text{ cm}^{-1}$  to  $3800\text{ cm}^{-1}$  and the Phobos relevant samples have been selected according to the Planetary Simulant Database (PCA-1 Phobos Captured Asteroid). The following typical mineral classes can be identified from Fig. 1(a): hydrated phyllosilicates (e.g. chrysotile, orange line); carbonates (e.g. calcium carbonate, violet line); pyroxene (e.g. diopside, green line and enstatite, red line); iron sulphide (e.g. pyrite, blue line); anhydrous silicates (e.g. olivine, yellow line) and iron oxides (e.g. hematite, light blue line). It is important to note, that the majority of the Raman peaks of all samples are observed in the spectral range of  $50\text{ cm}^{-1}$  to  $1200\text{ cm}^{-1}$ . Here, the primary Raman modes of most minerals are located. A prominent example are the Raman active modes of the sulphate anion, see Ref. [4]. Another important feature of Raman spectroscopy in the spectral range of up to  $3800\text{ cm}^{-1}$  is the capability to detect the presence of water in minerals. This becomes obvious from the spectrum of the chrysotile sample in Fig. 1(a). Here, a sharp Raman peak is observed at a Raman shift of  $3700\text{ cm}^{-1}$ , which can be assigned to a Raman active mode of its OH group. In addition, organic substances can be detected in the spectral range from  $1500\text{ cm}^{-1}$  to  $3000\text{ cm}^{-1}$ . An example is carbon with two Raman active modes peaking at  $1400\text{ cm}^{-1}$  and  $1600\text{ cm}^{-1}$  [not shown in Fig. 1(a)]. A detailed description of the related Raman modes covered by the RAX instrument spectral range is described in Ref. [5].

Although not relevant for the mission to Phobos, the spectral range of the RAX instrument also allows for the unambiguous identification of samples that indicate the possible existence of pure water and biologic material. A few examples are presented in Fig. 1(b). Here, the Raman spectra of water ice (blue line), gypsum (pink line) and carotene (green line) are plotted in the spectral range of  $50\text{ cm}^{-1}$  to  $3800\text{ cm}^{-1}$ . Again, the measurements were performed with the confocal WiTEC Raman system. The Raman modes of water ice appear as broad spectral bands in the range of  $150\text{ cm}^{-1}$  to  $300\text{ cm}^{-1}$  and  $2900\text{ cm}^{-1}$  to  $3600\text{ cm}^{-1}$ , respectively. The sample of gypsum contains the primary Raman modes of the sulphate anion in the spectral range of up to  $1200\text{ cm}^{-1}$  and two Raman modes related to the OH stretching vibrations at  $3400\text{ cm}^{-1}$  and  $3500\text{ cm}^{-1}$ . Carotene is a prominent biomarker present in terrestrial microorganisms with significant features at  $1000\text{ cm}^{-1}$ ,  $1200\text{ cm}^{-1}$  and  $1500\text{ cm}^{-1}$ . According to Ref. [6], these features can be identified as the C-CH<sub>3</sub> deformation as well as the C-C and C=C stretching modes.

### 3. RAX Instrument Design

The RAX instrument consists of two physically separated units, the RAX Laser Assembly (RLA) and the RAX Spectrometer Module (RSM). The RLA includes a Raman laser, which is based on a flight spare laser unit developed for the ExoMars2020 mission by Instituto Nacional de Técnica Aeroespacial (INTA) and University of Valladolid (UVa). A picture of the RLS laser unit is presented in Fig. 2. The laser, which has been optimized for efficient Raman excitation, provides an emission wavelength of 532 nm and an optical output power of up to 100 mW in the thermal operating range of  $+20$  to  $+30^\circ\text{C}$ . Since the laser linewidth defines the resolving power of the spectrometer, the laser temperature will be stabilized during RAX operations to an accuracy of  $\pm 0.1\text{ K}$  by a thermoelectric module, which is also part of the RLA. This corresponds to a laser linewidth stability of better than 0.1 nm, which is sufficient to resolve the spectral signatures of the minerals which are expected on Phobos. The RLA has a small mass of 66 g and covers a volume of only  $14 \times 55 \times 65\text{ mm}^3$ . The electrical power consumption without heating is approximately 2 W.

The RSM of the RAX instrument is used for controlling and interfacing the RLA. Both units are connected through an optical fibre (length:  $\sim 1\text{ m}$ ) with a core diameter of  $50\text{ }\mu\text{m}$  and a numerical aperture of 0.2. The RSM can be further subdivided into five subcomponents, the Spectrometer Optics (SPO), the Auto-Focus Subsystem (AFS), the Front Panel Assembly (FPA), the Laser Control Board (LCB) and the Auxiliary Electronics Board (AEB).

The SPO contains all optical components of the spectrometer except the laser. This includes five lens assemblies for beam collimation and focusing, the monochromator which is based on a slit with a width of

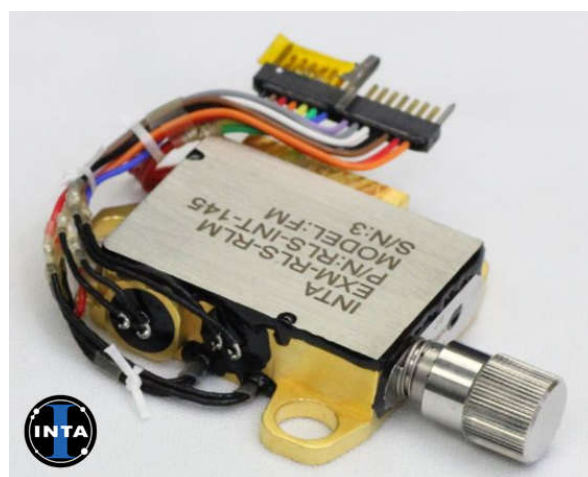


Fig. 2. Picture of the RLS laser flight spare unit used for ExoMars 2020 (Credit: INTA).

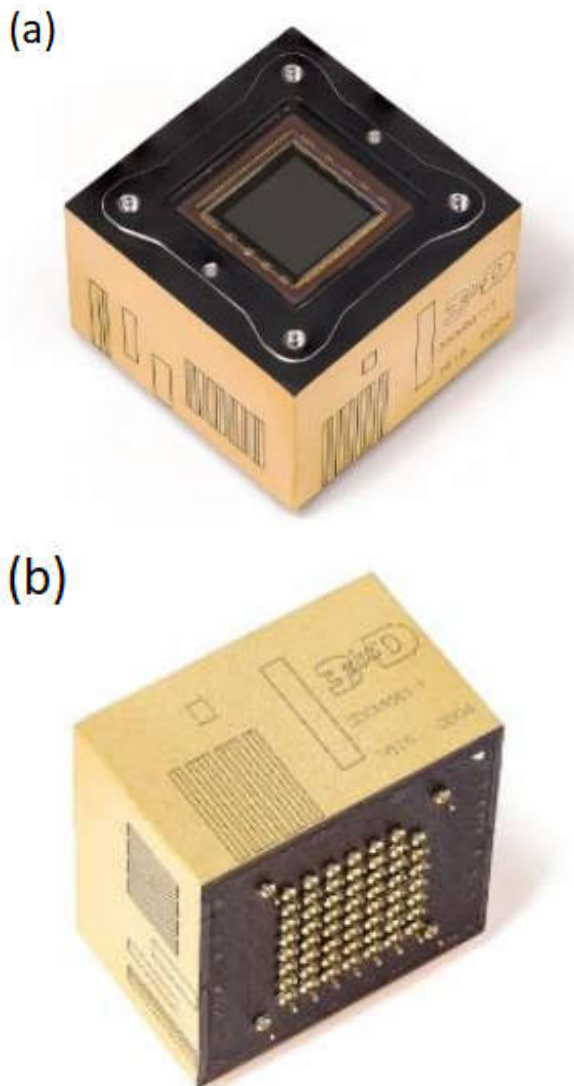


Fig. 3(a). Top and (b) bottom view of the CMOS space camera detector (3DCM734, 3Dplus). Taken from Ref. [8].

50  $\mu\text{m}$  and a volume phase holographic (VPH) grating, several mirrors and filters, and a space-qualified CMOS detector (3DCM734, 3Dplus). While the VPH grating technology provides a high diffraction efficiency which is superior to standard surface relief gratings [7], the detector enables a small system size with a mass of only 64 g and a volume of approximately  $35 \times 35 \times 23 \text{ mm}^3$  [8]. A picture of the detector top and bottom view is provided in Fig. 3(a) and (b). The CMOS sensor consists of  $2048 \times 2048$  pixels with a pixel pitch of 5.5  $\mu\text{m}$ . Each pixel is based on a pinned photodiode architecture with several transistors. Details of the camera design are described in Refs. [8,9]. The SPO provides a spectral resolution of approximately  $10 \text{ cm}^{-1}$  for the spectral range of up to  $4000 \text{ cm}^{-1}$ .

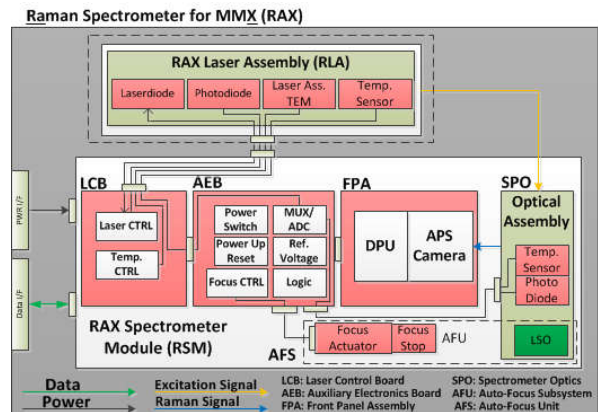


Fig. 4. Block diagram of the general RAX instrument architecture.

A key component of the RSM is the AFS. It comprises the Light Shuttle Objective (LSO), which is the movable entrance lens group inside the SPO for focusing the laser beam onto the Phobos ground to a waist diameter of approximately 50  $\mu\text{m}$ , and an autofocus unit (AFU). The AFU is based on a focus actuator that allows the SPO to adjust its working distance of 80 mm within a range of  $\pm 10 \text{ mm}$ . However, since the initial height above the Phobos ground is unknown, coarse autofocusing has to be realized with the MMX rover in the loop.

The RSM electronics includes the Front Panel Assembly (FPA), which contains the Digital Processing Unit (DPU) as well as the CMOS space camera detector. All components required to operate the camera, such as FPGA, voltage generation, memory, and circuit protection, are located in the DPU. The FPGA is used for controlling the detector and for control of the RAX instrument. In order to connect the AEB electronics directly to the FPGA, the camera module provides an interface (JTAG, GPIO, LVDS input and LVDS output). The AEB includes the subcomponents for housekeeping acquisition (voltages and temperatures), power switching, autofocus control and shift registers to extend the available GPIOs to the FPGA. It also provides an internal interface to the AFU. Directly connected to the AEB is the LCB. It consists of the laser controller and the temperature control electronics and provides a direct internal interface to the RLA.

A block diagram of the general RAX architecture is provided in Fig. 4. Here, the dashed lines indicate the instrument parts which are provided by DLR project partners. This concerns the RLA, which is provided by INTA/University of Valladolid (UVa) and the AFS as a part of the RSM, which is provided by JAXA/University of Tokyo (UTo), respectively. A model of the preliminary design of the RAX instrument

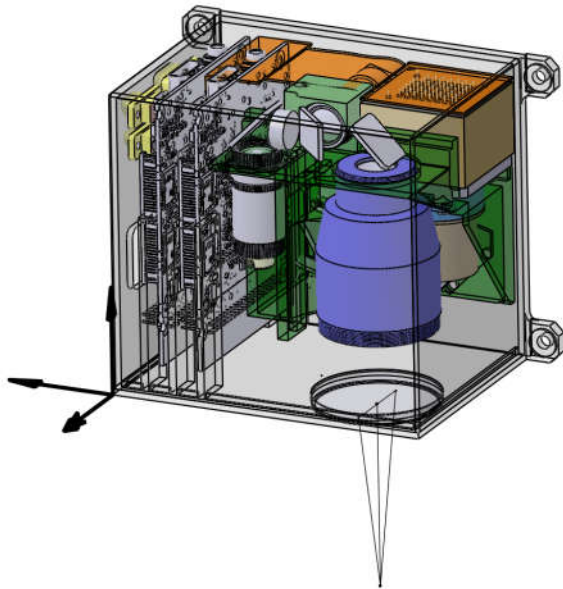


Fig. 5. Preliminary design of the RSM with a volume of  $81 \times 125 \times 98 \text{ mm}^3$  and a mass of  $<1.4 \text{ kg}$ .

is shown in Fig. 5. The blue and green components highlight the AFS and some mounting structure of the SPO. The black lines at the bottom of the RSM indicate the focused laser beam with an expected working distance of 80 mm, calculated from the LSO entrance lens to the soil of Phobos. The FPA and the detector are indicated by the orange components in Fig. 5, which are connected to the AEB via flex harness. Next to the LCB, on the left side of the RSM, several connectors are highlighted in yellow color, providing an electrical and optical interface to the RLA, as well as a power and SpaceWire interface to the MMX rover.

#### 4. RAX Breadboard Model

Raman measurements were performed with a breadboard model at DLR-OS to test the preliminary RAX optical design performance. Figure 6 presents a schematic of the optical system. Visible radiation at an emission wavelength of 532 nm is generated by a frequency-doubled Nd:YAG laser, which is coupled to the breadboard with an optical fibre. The beam is collimated by a first objective, the fibre input collimator and incides on a beam splitter (splitting ratio: 90:10). While a small fraction of the laser light is coupled out for measuring the laser power and for focusing test purposes, most of the collimated beam passes the autofocus objective, which corresponds to the LSO in the RAX instrument. The autofocus objective is mounted onto a translation stage driven by a stepper motor in order to account for the AFU present in the instrument. It focuses the beam onto the sample, in this

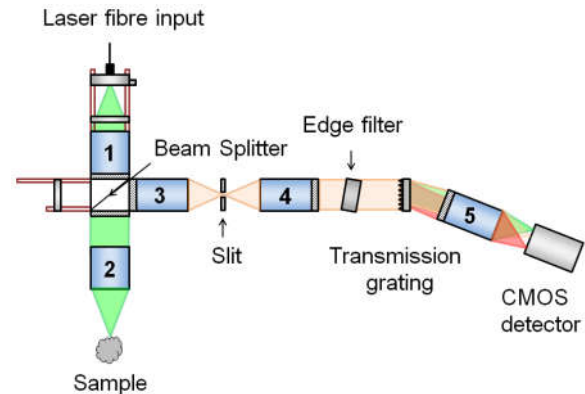


Fig. 6. Scheme of the experimental setup used for Raman spectroscopy (Breadboard Model). The visible radiation is generated by a frequency-doubled Nd:YAG laser with an emission wavelength of 532 nm, which is coupled to the breadboard via an optical fibre. The optical path consists of five consecutively numbered objectives for beam collimation and focusing, a beam splitter, a monochromator based on a transmission grating, and an edge filter for cancelling the light that is not related to the Raman effect. For autonomous focusing of the laser light onto the sample, the second objective is mounted onto a translation stage driven by a stepper motor. The focus is obtained by software evaluation of the images that are taken during illumination of the scene with an LED. The inelastically scattered Raman light is separated at the grating and focused into a CMOS detector. Note that for the spectrum provided in Fig. 7, a performance equivalent model of the RLS laser unit has been employed as a laser source. 1: Fibre input collimator; 2: Autofocus objective (corresponds to LSO); 3: Slit entrance objective; 4: Slit output objective; 5: Camera interface objective.

case  $\text{CaSO}_4 \times 2\text{H}_2\text{O}$  (gypsum). In order to autonomously perform the best focus position, contrast images generated by the oblique incidence of an LED are evaluated by a software algorithm prior to a measurement of a new sample. Once the sample is in focus, the Raman effect can be exploited to record spectra of the sample. The inelastically scattered Raman light is reflected at the beam splitter onto the slit entrance objective, which focuses the light onto the 50  $\mu\text{m}$  wide slit. Behind the slit, the diverging beam is re-collimated by the slit output objective and impinges on an edge filter for cancelling the laser light that does not originate from Raman scattering. The transmitted Raman photons are spatially separated by the dispersion at the transmission grating. Finally the light is focused onto the CMOS detector by the camera interface objective.

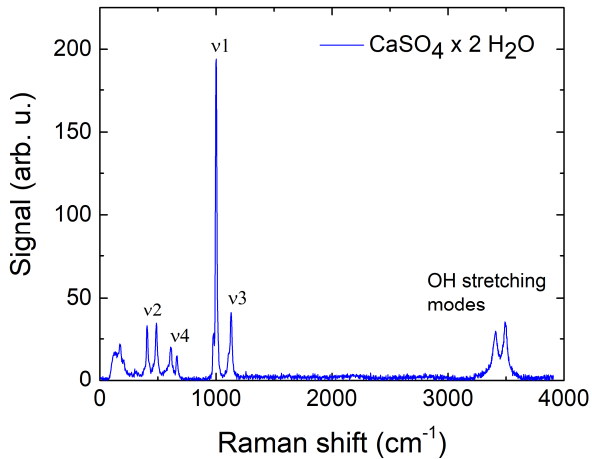


Fig. 7. Raman spectrum of a  $\text{CaSO}_4 \times 2\text{H}_2\text{O}$  (gypsum) sample obtained at the RAX breadboard model. The measurement has been performed using a performance equivalent model of the RLS laser unit and a standard CMOS detector based on the same sensor as the 3D-Plus space camera. The wavenumber scale has been derived by spectral calibration of the detector with the emission spectrum of a neon lamp.

Figure 7 shows the Raman spectrum of a  $\text{CaSO}_4 \times 2\text{H}_2\text{O}$  (gypsum) sample, which has been measured at the RAX breadboard model at room temperature. The sample has been illuminated by a performance equivalent RLS laser unit with a laser power of approximately 15 mW on the sample. As a detector, we have employed a commercial CMOS camera (Mako G-419B POE, Allied Vision), which uses an identical sensor as the selected 3D-Plus space camera. Due to the dispersion at the grating, the Raman spectra appear as a spatial distribution with local intensity maxima on the sensor. A cross-section of the image can then be evaluated in order to obtain a spectrum. In this case, sixty camera images were averaged in order to improve the signal-to-noise ratio (SNR). Each picture was measured with an integration time of 1 s. The wavelength scale was derived by a spatial-spectral assignment of the camera pixels to the emission spectrum of a neon light bulb.

In the Raman spectrum in Fig. 7, several Raman peaks are observed in the spectral range of up to  $1200 \text{ cm}^{-1}$ . According to Ref. [4], these peaks are identified as the sulphate anion vibrational modes v1 (non-degenerated symmetric stretching mode), v2 (double degenerated bending vibration), v3 (threefold degenerated anti-symmetric stretching mode), and v4 (threefold degenerated bending vibration). In the spectral range of  $3400 \text{ cm}^{-1}$  to  $3500 \text{ cm}^{-1}$  another two Raman peaks are observed, which can be assigned to the OH stretching modes according to Ref. [5]. The maximum SNR of approximately 100 is obtained for the v1 Raman line. However, further improvements on the

SNR are expected here by increasing the integration time to several seconds and by reducing the detector dark noise current, which can be realized by decreasing the sensor temperature to the operational environment.

### 5. RAX onboard the MMX rover

The MMX rover for Phobos is a joint contribution by CNES and DLR to JAXA's Martian Moons Exploration mission [10]. Currently, the rover weighs 29.1 kg and contains two navigation cameras (NavCam), two wheel cameras (WheelCam) and a radiometer (miniRad) in addition to the RAX instrument. The entire payload mass is approximately 2.6 kg. A more detailed description of the rover system design is provided in Ref. [11]. The RAX instrument is part of the internal module (service module, SEM) within the MMX rover. A current model of the rover design is shown in the front and top view in Fig. 8(a) and (b). The accommodation of the RLA (red arrow) and the RSM (blue arrow) in the SEM is indicated in Fig. 8(a). The RSM is located right next to the rover front wheel camera, which employs a 3D Plus space camera similar to that of the RAX instrument. The red

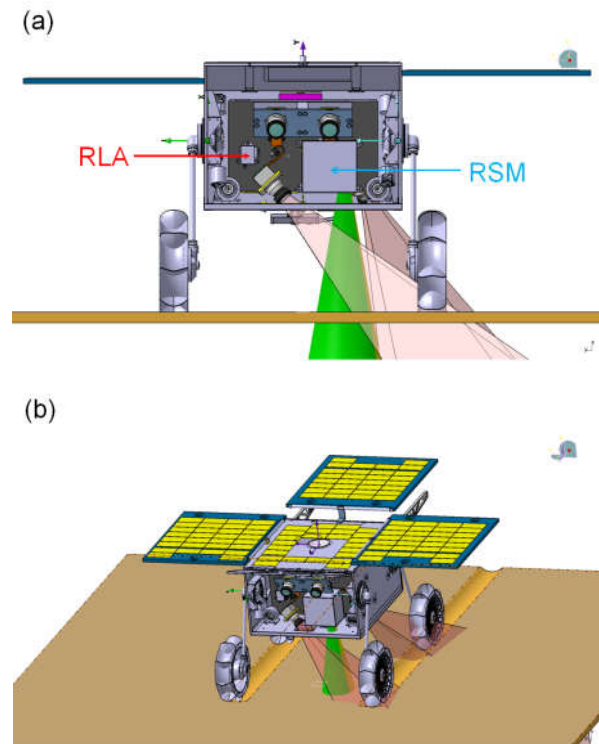


Fig. 8(a). Front and (b) top view of the current MMX rover design with the RAX instrument onboard the SEM. The two units RLA and RSM are indicated by the red and blue arrow in Fig. 8(a), respectively. The green cone indicates the FOV of the RAX instrument. (Credit: CNES/DLR)

and green cones below the SEM are indicating the field of views (FOVs) of the front wheel camera and the RAX instrument, respectively. As can be seen, there is an overlap of the two FOVs. The front wheel camera is able to capture an image of the scene which RAX is going to examine. This might have significant advantages in the evaluation of the recorded data, since the Raman spectra can be directly compared with an environmental image for context information.

In order to avoid the influence of ambient light, the measurements of the RAX instrument are performed during Phobos night. Before switching on RAX, the rover lowers in several iterations to an initial height of 70 mm to 90 mm relative to the soil of Phobos. In this regime, the RAX instrument can realize autonomous autofocusing with the AFS. After RAX is turned on, a first autofocus sequence is performed with an LED. This procedure is similar to that performed at the breadboard model. Then the laser is turned on and set to the desired current-temperature operating point, which defines the optical power irradiated onto the sample. Because of the laser frequency tunability with temperature, accurate stabilization of the laser temperature is necessary and will be realized by a thermoelectric module. Once the laser is stabilized, the Rayleigh light, which is not suppressed by the edge filter, can be used to achieve precise fine adjustment of the instruments working distance. Thereafter, RAX enters the science mode where the Raman measurements are performed. Several spectra of a sample are recorded and processed onboard. In order to provide frequency calibration of the instrument, a calibration target is foreseen to be part of the rover. The typical amount of data per measurement that will be downlinked to Earth is on the order of 100 kB. The maximum power consumption of up to 10 W without laser heating is obtained during the instruments focusing mode. After completion of the measurement, the laser and the spectrometer units are switched off.

By rover movement, different locations on the surface of Phobos can be selected for measurements, which allows for the investigation of the moon's surface heterogeneity. Currently the goal is to drive up to 100 m during hundred days on Phobos. Since the beam diameter of the RAX instrument on the sample is approximately 50  $\mu\text{m}$ , a large variety of data can be collected even with much shorter driving distances. In addition, as soon as the rover moves to the MMX landing site, the traces of the MMX lander can be analysed by RAX.

## 6. Conclusions and Outlook

We are developing a high compact and lightweight Raman spectrometer for the MMX rover mission to Phobos. By exploiting the Raman effect, which is based on inelastic photon scattering, the spectrometer is

capable of the unique identification and structural analysis of substances, such as water-bearing minerals and organics in the spectral range of up to 4000  $\text{cm}^{-1}$  with a resolution of 10  $\text{cm}^{-1}$ . First results obtained from a breadboard model confirm our optical design performance. The whole RAX instrument requires a volume of approximately  $81 \times 125 \times 98 \text{ mm}^3$  and has a mass of less than 1.4 kg.

The RAX project, which is currently in its Phase B, is a major scientific international cooperation between JAXA/UTo, INTA/UVa and DLR-OS, respectively. The RAX Flight Model will be delivered to the rover in 2022 and the MMX mission is to be launched in 2024. RAX operations on Phobos are currently foreseen for several days at the beginning of 2027. The Raman spectra recorded by RAX allow for the determination of the surface mineralogy on Phobos which is a top-level science goal as defined by JAXA. Furthermore, a comparison of the RAX data with the results obtained by the RLS instrument during the ExoMars rover mission opens the path for revealing the origin of Mars and one of its moons.

## Acknowledgements

MMX is a JAXA mission with contributions from NASA, CNES and DLR. The MMX rover will be provided by CNES and DLR. The RAX instrument is a joint development from JAXA/UTo, INTA/UVa and DLR-OS.

The authors would like to thank the teams of MMX, the rover and the RAX instrument as well as the programmatic support to start this project.

## References

- [1] S. M. Angel, N. R. Gomer, S. K. Sharma, and C. McKay, Remote Raman spectroscopy for planetary exploration: a review, *Appl. Spectrosc.* 66 (2012) 137–150.
- [2] R. C. Wiens, S. Maurice, and F. Rull Perez, The SuperCam remote sensing instrument suite for the Mars2020 rover mission: A preview. *Spectroscopy* 32 (2017) LA–UR–17–26876.
- [3] F. Rull, S. Maurice, I. Hutchinson, A. Moral, C. Perez, C. Diaz, M. Colombo, T. Belenguer, G. Lopez-Reyes, A. Sansano, O. Forni, Y. Parot, N. Striebig, S. Woodward, C. Howe, N. Tarcea, P. Rodriguez, L. Seoane, A. Santiago, J. A. Rodriguez-Prieto, J. Medina, P. Gallego, R. Canchal, P. Santamaria, G. Ramos, J. L. Vago, On behalf of the RLS team, The Raman laser spectrometer for the ExoMars Rover mission to Mars, *Astrobiology* 17 (2017) 627–654.
- [4] K. Ben Mabrouk, T. H. Kauffmann, H. Aroui, and M. D. Fontana, Raman study of cation effect on sulfate vibration modes in solid state and in aqueous



- solutions, *J. Raman Spectrosc.* 44 (2013) 1603–1608.
- [5] F. Rull, S. Maurice, E. Diaz, C. Tato, A. Pacros, and the RLS Team, The Raman Laser Spectrometer (RLS) on the Exomars 2018 Rover Mission, 42<sup>nd</sup> Lunar and Planetary Science Conference, The Woodlands, Texas, USA, 2011, 7 – 11 March.
- [6] V. E. de Oliveira, H. V. Castro, H. G. M. Edwards, and L. F. C. de Oliveira, Carotenes and carotenoids in natural biological samples: a Raman spectroscopic analysis, *J. Raman Spectrosc.* 41 (2010) 642–650.
- [7] J. Loicq, L. M. Venancio, Y. Stockman, and M. P. Georges, Performances of volume phase holographic grating for space applications: study of the radiation effect, *Appl. Opt.* 52 (2013) 8338–8346.
- [8] C. Sellier, D. Gambart, N. Perrot, E. Garcia-Sanchez, C. Virmontois, W. Mouallem, and A. Bardoux, Development and qualification of a miniaturized CMOS Camera for Space Applications (3DCM734/3DCM739), International Conference on Space Optics – ICSO 2018, Chania, Greece, 2018, 9 – 12 October.
- [9] C. Sellier, D. Gambart, N. Perrot, E. Garcia-Sanchez, C. Virmontois, and A. Bardoux, CMOS Camera for Space Applications (3DCM681), International Conference on Space Optics – ICSO 2016, Biarritz, France, 2016, 16 – 21 October.
- [10] T. Usui, K. Kuramoto, and Y. Kawakatsu, Martian Moons eXploration (MMX): Japanese Phobos Sample Return Mission, 42<sup>nd</sup> COSPAR Scientific Assembly, Pasadena, California, USA, 2018, 14 – 22 July.
- [11] S. Ulamec, P. Michel, M. Grott, U. Böttger, H.-W. Hübers, N. Murdoch, P. Vernazza, Ö. Karatekin, J. Knollenberg, K. Willner, M. Grebenstein, S. Mary, P. Chazalnoel, J. Biele, C. Krause, T.-M. Ho, C. Lange, J. T. Grundmann, K. Sasaki, M. Maibaum, O. Küchemann, J. Reill, M. Chalon, S. Barthelmes, R. Lichtenheldt, R. Krenn, M. Smisek, J. Bertrand, A. Moussi, C. Delmas, S. Tardivel, D. Arrat, F. Ijpelaan, L. Melac, L. Lorda, E. Remeteau, M. Lange, O. Mierheim, S. Reershemius, T. Usui, M. Matsuoka, T. Nakamura, K. Wada, H. Miyamoto, K. Kuramoto, J. LeMaitre, G. Mas, M. Delpech, L. Celine, A. Rafflegeau, H. Boirard, R. Schmisser, C. Virmontois, C. Cenac-Morthe, and D. Besson, A Rover for the JAXA MMX Mission to Phobos, IAC-19-A3.4.8, 70<sup>th</sup> International Astronautical Congress, Washington DC., USA, 2019, 21 – 25 October.